

Patient-specific and gene-corrected induced pluripotent stem cell-derived endothelial cells elucidate single-cell phenotype of pulmonary veno-occlusive disease

Baihui Ma,¹ Tianjiao Li,¹ Wenke Li,¹ Hang Yang,¹ Qixian Zeng,² Zihang Pan,³ Kai Wang,³ Qianlong Chen,¹ Changming Xiong,^{2,*} and Zhou Zhou^{1,*}

¹State Key Laboratory of Cardiovascular Disease, Beijing Key Laboratory for Molecular Diagnostics of Cardiovascular Diseases, Diagnostic Laboratory Service, Fuwai Hospital, National Center for Cardiovascular Diseases, Chinese Academy of Medical Sciences and Peking Union Medical College, Beijing 100037, China

²State Key Laboratory of Cardiovascular Disease, Center of Pulmonary Vascular Disease, Fuwai Hospital, National Center for Cardiovascular Disease, Chinese Academy of Medical Sciences and Peking Union Medical College, North Lishi Road, Xicheng District, No.167, Beijing, China

³Department of Physiology and Pathophysiology, School of Basic Medical Sciences, Peking University; Key Laboratory of Molecular Cardiovascular Science, Ministry of Education, Beijing 100191, China

*Correspondence: xiongmfw@163.com (C.X.), zhouzhou@fuwaihospital.org (Z.Z.)

<https://doi.org/10.1016/j.stemcr.2022.10.014>

SUMMARY

Pulmonary veno-occlusive disease (PVOD) is a rare form of pulmonary hypertension characterized by the preferential remodeling of the pulmonary venules. Hereditary PVOD is caused by biallelic variants of the *EIF2AK4* gene. Three PVOD patients who carried the compound heterozygous variants of *EIF2AK4* and two healthy controls were recruited and induced pluripotent stem cells (iPSCs) were generated from human peripheral blood mononuclear cells (PBMCs). The *EIF2AK4* c.2965C>T variant (PVOD#1), c.3460A>T variant (PVOD#2), and c.4832_4833insAAAG variant (PVOD#3) were corrected by CRISPR-Cas9 in PVOD-iPSCs to generate isogenic controls and gene-corrected-iPSCs (GC-iPSCs). PVOD-iPSC-endothelial cells (ECs) exhibited a decrease in GCN2 protein and mRNA expression when compared with control and GC-ECs. PVOD-ECs exhibited an abnormal EC phenotype featured by excessive proliferation and angiogenesis. The abnormal phenotype of PVOD-ECs was normalized by protein kinase B inhibitors AZD5363 and MK2206. These findings help elucidate the underlying molecular mechanism of PVOD in humans and to identify promising therapeutic drugs for treating the disease.

INTRODUCTION

Pulmonary veno-occlusive disease (PVOD) is a rare and devastating cause of pulmonary hypertension (PH) (Montani et al., 2016), which results in the progressive increase in pulmonary vascular resistance, culminating in right heart failure and death (Simonneau et al., 2013). The pulmonary venous system is primarily involved in PVOD, which is characterized by significant pulmonary capillary dilatation and intense proliferation (Mandel et al., 2000; Montani et al., 2009). Through specific pulmonary arterial hypertension (PAH) therapy treatment, PVOD can be characterized by poor prognosis and the possibility of developing severe pulmonary edema. Lung transplantation is the destination therapy for eligible patients (Montani et al., 2016). To date, PVOD remains a poorly understood entity. Thus, identifying the critical pathophysiological mechanisms in mediating pulmonary capillary remodeling would be pivotal for inhibiting and reversing PVOD. The dysfunction of pulmonary endothelial cells (ECs) plays a central role in the initiation and progression of PVOD. Microvascular EC proliferation can be observed in both lung tissues of PVOD patients and the mitomycin-induced rat PVOD model (Perros et al., 2015).

In 2014, the French PH network reported the genealogy of 13 PVOD families with heritable disease, which pointed to eukaryotic translation initiation factor 2 alpha kinase 4 (*EIF2AK4*) as a major gene that is linked to PVOD development (Eyries et al., 2014). Furthermore, the 2015 ESC/ERS guidelines recommend that the presence of biallelic variants of *EIF2AK4* is sufficient to confirm the diagnosis of PVOD, without performing a hazardous lung biopsy for histological confirmation (Galiè et al., 2016). The *EIF2AK4* gene codes for general control nonderepressible 2 (GCN2), which belongs to the family of four kinases that phosphorylate the α -subunit of eukaryotic translation initiation factor 2 (eIF2 α). GCN2 has been demonstrated to be involved in responses to other triggers, including viral infections, hypoxia, and UV radiation (Donnelly et al., 2013). The expression of GCN2 decreases in pulmonary tissues of PVOD patients (Perros et al., 2015). Heme oxygenase 1 (HO-1) and CCAAT-enhancer-binding protein (C/EBP) homologous protein (CHOP) were reported as the two downstream effectors of GCN2 signaling and ER stress in rat PVOD samples (Manaud et al., 2020). However, there is limited knowledge on how *EIF2AK4* biallelic variants cause PVOD in humans.

Induced pluripotent stem cells (iPSCs) made from human adult cells by defined transcription factors can be



differentiated into functional cells of different lineages. This provides a promising cell source for translational and regenerative medicine (Guo et al., 2019; Matsa et al., 2014), and it opens an exciting avenue for the generation of patient-specific ECs for cardiovascular disease-modeling and therapeutics. iPSCs can capture the genetic diversity of the patients and are particularly useful for exploring the disease pathogenesis caused by complex genetic variants. Using human-based and patient-specific iPSC-ECs as cellular models, the underlying mechanisms of the human cardiac disease phenotype can be observed, and therapeutic compounds can be screened. Disease-specific iPSC-ECs have been generated and applied to investigate the PAH caused by the bone morphogenetic protein receptor type II (BMPR2) variant (Gu et al., 2017).

The present study generated iPSC lines from three PVOD patients who carried *EIF2AK4* variants (PVOD#1: c.2965C>T and c.4724T>C; PVOD#2: c.4736T>C and c.3460A>T; PVOD#3: c.1942A>T and c.4832_4833insAAAG) and two healthy control subjects. Using CRISPR-Cas9 genome-editing technology, the GC-PVOD-iPSC lines were generated as isogenic controls, and the p.Arg989Trp variant (c.2965C>T), p.Lys1154Ter variant (c.3460A>T) and p.Pro1611fs variant (c.4832_4833insAAAG) were corrected. Then, control-iPSC-ECs, PVOD-iPSC-ECs, and GC-PVOD-iPSC-ECs were successfully generated. Afterward, the GCN2 expression, proliferation, and angiogenesis of iPSC-ECs and gene expression profile were compared to determine the mechanism of PVOD at the cellular level and, further, to verify whether AKT inhibitors imatinib and amifostine can effectively rescue the dysfunctional EC phenotype of PVOD.

RESULTS

Clinical characteristics

The recruited PVOD#1 patient was a 39-year-old female, the recruited PVOD#2 patient was a 26-year-old male, and the recruited PVOD#3 patient was a 42-year-old female. These patients exhibited a reduced diffusing lung capacity of carbon monoxide, severe pre-capillary PH, interlobular septal thickening and mediastinal lymphadenopathy, and centrilobular ground-glass opacification (Figure 1A). These patients were initially diagnosed with PAH, and the genetic screening of PAH-related genes (*BMPR2*, *KCNK3*, *CAV1*, *SMAD9*, *BMPR1B*, *ACVRL1*, *ENG*, *GDF2*, *SMAD4*, *EIF2AK4*, *KCNA5*, *NOTCH3*, and *TOPBP1*) revealed the compound heterozygous variants in the *EIF2AK4* gene pore region of these patients (Figure S1B). The details for the mutations information are presented in Figure 1B. According to the ESC/ERS guidelines, these patients were categorized as having PVOD. The two mutant sites of these patients were inherited from their father and mother, respectively. The PVOD#1 patient has a brother who carries the R989W mutation but does not present any signs of PVOD (Figure S1A). The two healthy control subjects included a 32-year-old male and a 22-year-old female. These subjects had no history of heart disease, serious infections, or obvious genetic diseases (Yang et al., 2018).

denopathy, and centrilobular ground-glass opacification (Figure 1A). These patients were initially diagnosed with PAH, and the genetic screening of PAH-related genes (*BMPR2*, *KCNK3*, *CAV1*, *SMAD9*, *BMPR1B*, *ACVRL1*, *ENG*, *GDF2*, *SMAD4*, *EIF2AK4*, *KCNA5*, *NOTCH3*, and *TOPBP1*) revealed the compound heterozygous variants in the *EIF2AK4* gene pore region of these patients (Figure S1B). The details for the mutations information are presented in Figure 1B. According to the ESC/ERS guidelines, these patients were categorized as having PVOD. The two mutant sites of these patients were inherited from their father and mother, respectively. The PVOD#1 patient has a brother who carries the R989W mutation but does not present any signs of PVOD (Figure S1A). The two healthy control subjects included a 32-year-old male and a 22-year-old female. These subjects had no history of heart disease, serious infections, or obvious genetic diseases (Yang et al., 2018).

Generation and characterization of PVOD-iPSCs and GC-PVOD-iPSCs

PVOD-iPSCs and control-iPSCs were generated from peripheral blood mononuclear cells (PBMCs) derived from three PVOD patients and two healthy control subjects through the nonintegrated Sendai-viral transduction of reprogramming factors (*OCT3/4*, *SOX-2*, *KLF-4*, and *C-MYC*). Since the biallelic mutations of the *EIF2AK4* gene can cause heritable PVOD, and the heterozygous mutation remains insufficient (Eyries et al., 2014), the p.Arg989Trp variant (c.2965C>T), p.Lys1154Ter variant (c.3460A>T), and p.Pro1611fs variant (c.4832_4833insAAAG) were corrected using the CRISPR-Cas9 system with ssODNs as the isogenic controls for PVOD-iPSCs (Figure 1C). All three iPSC lines exhibited typical human pluripotent stem cell-like morphologies (Figure S1C). The immunofluorescence staining revealed that most of the cells were positive for *NANOG*, *OCT4*, *SSEA-1*, and *TRA-1* (Figure S2A). The normal karyotypes of PVOD-iPSCs are presented in Figure S2B. This was also verified by regular real-time qPCR, while probing for pluripotency markers (Figure S2D). The *EIF2AK4* compound heterozygous variants were further validated by genetic workup in all iPSC lines (Figure 1D), and the cell line was not contaminated with mycoplasma (Figure S2C).

Figure 1. Generation and characterization of PVOD patients-specific induced pluripotent stem cells (iPSCs) and gene-corrected PVOD-iPSCs (GC-PVOD-iPSCs)

- (A) The high-resolution computed tomography (CT) of the chest from three PVOD patients showed significant centrilobular ground-glass opacification (The red arrows indicated) and interlobular septal thickening.
- (B) The *EIF2AK4* mutation sites information in three PVOD patients and their pathogenicity classification. VUS means uncertain significance, and LP means likely pathogenic.
- (C) Strategy of correcting *EIF2AK4* c.2965 C>T (PVOD#1) variant, c.3460A>T variant (PVOD#2), and c.4832_4833insAAAG variant (PVOD#3). The homologous sequences are shown between the red lines.
- (D) DNA sequencing demonstrates variant sites on *EIF2AK4* (PVOD#1: c.2965C>T and c.4724T>C; PVOD#2: c.4736T>C and c.3460A>T; PVOD#3: c.1942A>T and c.4832_4833insAAAG) of the three iPSC lines.

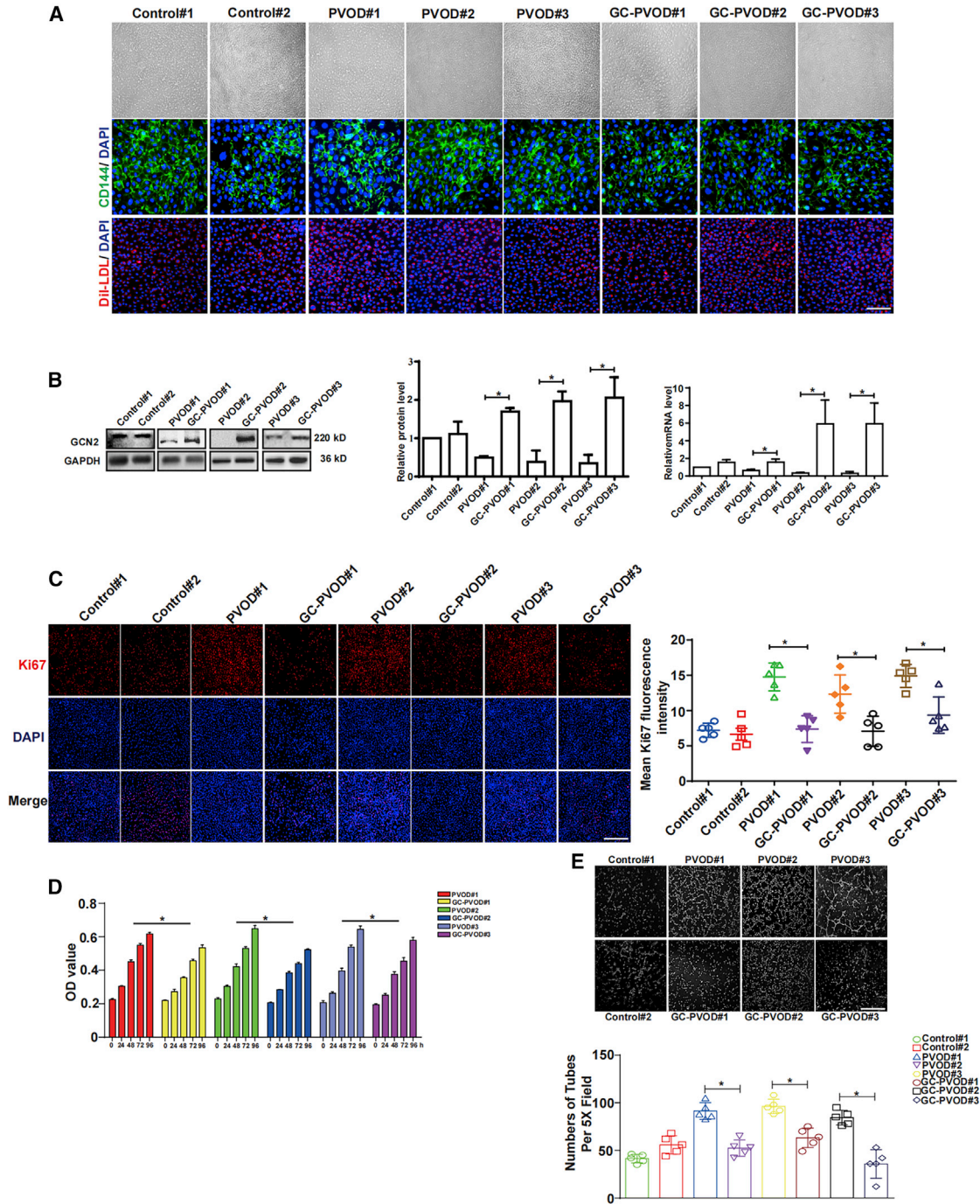


Figure 2. Excessive angiogenesis and proliferation of PVOD patients induced pluripotent stem cell-derived endothelial cells (PVOD-iPSC-ECs)

(A) Endothelial cells (ECs) differentiated from control, gene-corrected (GC), and PVOD-iPSCs exhibit typical cobblestone morphology, incorporate 3,3'-dioctadecylindocarbocyanine labeled low-density lipoprotein (DiI-LDL, red), and are positive for the EC surface marker CD144 (green). Blue: DAPI. Scale bar represents 100 μ m (top), 200 μ m (middle), and 200 μ m (bottom).

(B) *EIF2AK4* gene expression quantified by western blot and densitometric quantification of GCN2 protein and real-time qPCR in iPSC-ECs from controls, PVODs, and GCs. * $p < 0.05$ by one-way ANOVA followed by the Bonferroni test.

(C) Representative images of Ki67 immunostaining and quantitative data to compare the proliferation capacity of iPSC-ECs from controls, PVODs, and GCs. Scale bar, 50 μ m. * $p < 0.05$ by one-way ANOVA followed by the Bonferroni test.

(legend continued on next page)



Differentiation and characterization of iPSC-ECs

The three iPSC lines were differentiated into ECs, according to a monolayer differentiation protocol (Paik et al., 2018). This comprised three key steps: mesoderm induction, endothelial specification, and EC purification (Figure S3A). All groups of iPSC-ECs obtained from the three subjects exhibited similar EC cobblestone morphologies, a positive *CD144* (VE-cadherin) immunostaining, and an acetylated LDL uptake (Figure 2A). There were no significant differences in cell size among the control-iPSC-ECs, PVOD-iPSC-ECs, and GC-PVOD-iPSC-ECs. Next, western blot and real-time qPCR were performed to determine the effect of compound heterozygous variants on the *EIF2AK4* gene expression. As shown in Figure 2B, PVOD-iPSC-ECs had a significant low level of endogenous GCN2 protein and *EIF2AK4* mRNA, when compared with those in control-iPSC-ECs. However, the GCN2 expression was rescued in GC-PVOD-iPSC-ECs.

Excessive cell proliferation and angiogenesis in PVOD-iPSC-ECs

In clinic, PVOD patients suffer from abnormal exuberant pulmonary capillary dilatation and proliferation. Therefore, relative functional experiments were performed to determine whether PVOD-iPSC-ECs can recapitulate the disease phenotype *in vitro*. A significant increase in Ki67 positive immunostaining was observed in PVOD-iPSC-ECs, when compared with control-iPSC-ECs and GC-PVOD-iPSC-ECs (Figure 2C). Furthermore, the MTT assay revealed an increase in cell count of PVOD-iPSC-ECs, when compared with GC-PVOD-iPSC-ECs (Figure 2D). These data clearly indicate that *EIF2AK4* compound heterozygous variants regulate EC proliferation. This is consistent with a previous finding, in which mitomycin (MMC)-exposed PVOD rat lungs presented areas of exuberant microvascular endothelial cell proliferation (Fabrice et al., 2015). Tube formation assay is one of the most widely used *in vitro* assays to model the reorganization of angiogenesis, which plays a critical role in microvascular growth (Fabrice et al., 2015). As shown in Figure 2E, PVOD-iPSC-ECs had a more aggressive tube formation capacity, when compared with the other lines, indicating that the angiogenesis involved in the pathogenesis of PVOD was caused by the *EIF2AK4* compound heterozygous variants. Overall, these present findings distinctly demonstrate that the abnormal endothelial cell phenotype in PVOD-iPSC-ECs is featured by excessive cell proliferation and angiogenic

variability, and that the correction of *EIF2AK4* variants is requisite to fully normalize the EC dysfunction.

EIF2AK4 knockdown results in elevated proliferation and angiogenesis in HUVECs

Next, the *EIF2AK4* small interfering RNA (siRNA) was transfected into human umbilical vein endothelial cells (HUVECs) to further confirm whether *EIF2AK4* gene defects trigger the EC disease phenotype. The *EIF2AK4* mRNA and GCN2 protein levels remarkably decreased in the *EIF2AK4* siRNA group, when compared with the scrambled siRNA group (Figures 3A and 3B). Consistent with a previous finding on PVOD-iPSC-ECs, the *EIF2AK4* gene silencing led to immoderate proliferation and angiogenesis, when compared with the scrambled siRNA group, as determined by the MTT assay, Ki67-incorporation assay, and tube formation assay (Figures 3C–3E). Indeed, as a kinase that phosphorylates the α -subunit of eukaryotic translation initiation factor 2 (eIF2 α), GCN2 is involved in the control of the general translation in response to various cellular stresses by reducing protein synthesis and regulating changes in expression of genes involved in stress responses, which is defined as the “integrated stress response” (Castilho et al., 2014; Donnelly et al., 2013). The decrease in GCN2 expression disequilibrates the homeostasis, which may contribute to the intemperate expression of genes in proliferation and angiogenesis. These results on HUVECs are consistent with that in rat pulmonary artery ECs with GCN2 inhibitor treatment (Manaud et al., 2020). Overall, these findings indicate that the downregulation of the *EIF2AK4* expression is correlated with the EC aberrant proliferation and angiogenic phenotype.

EIF2AK4 biallelic variants increase cell cycle and angiogenesis genes in PVOD-iPSC-ECs

Next, RNA sequencing (RNA-seq) was carried out to identify the changes in gene expression between the three PVOD-iPSC-EC lines and the three GC-PVOD-iPSC-EC lines. There were 16,742 upregulated genes and 15,485 downregulated genes in GC-PVOD-iPSC-ECs when compared with PVOD-iPSC-ECs (Figure 4A). In accordance with the findings on the PVOD-iPSC-ECs phenotype, the KEGG (Kyoto Encyclopedia of Genes and Genomes) analysis revealed that the regulated genes that were enriched in gene terms were mainly correlated with pathways on cancer, the cell cycle, and the phosphatidylinositol

(D) MTT assay was conducted to evaluate the proliferation capacity of iPSC-ECs from control, PVODs, and GCs during a 4-day time period. * $p < 0.05$ by two-way ANOVA followed by Bonferroni post hoc test.

(E) Representative images of tube formation of iPSC-ECs from control, PVOD, and GC with quantitative analysis, indicating the number of tubes formed 6 h after seeding cells on Matrigel. Scale bar, 100 μm . Three independent experiments were performed in duplicate.

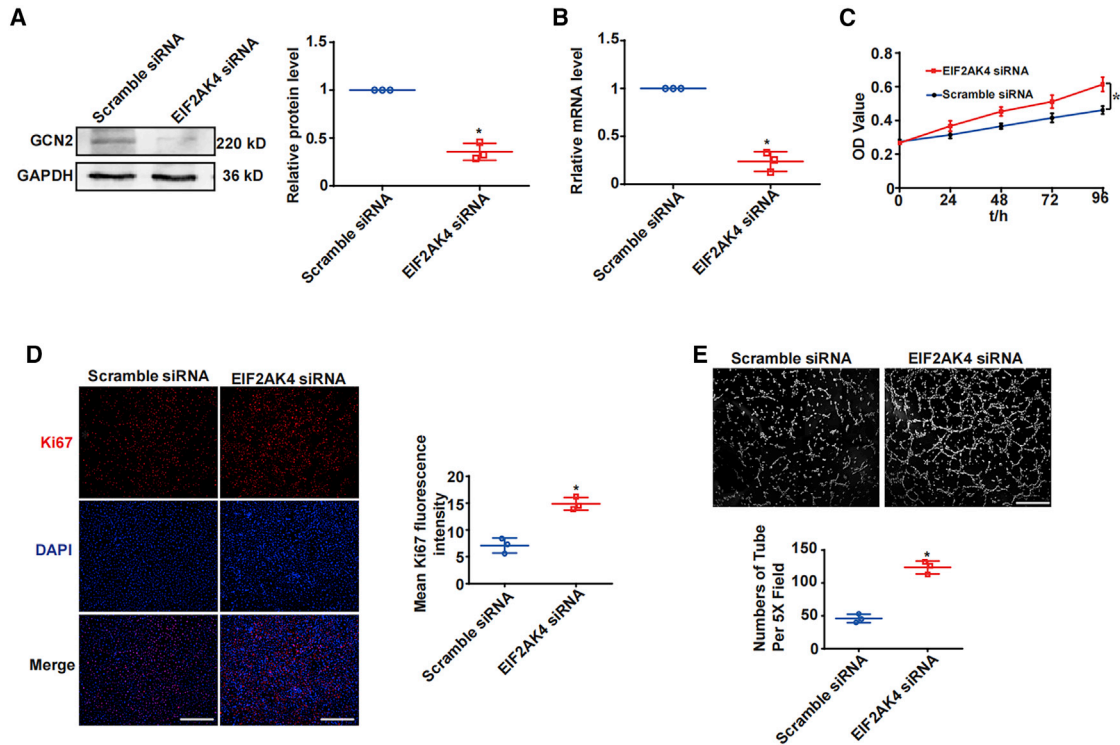


Figure 3. Disrupted proliferation and angiogenesis phenotype in HUVECs with *EIF2AK4* siRNA knockdown treatment

(A and B) Western blot and real-time qPCR show *EIF2AK4* expression in HUVECs with *EIF2AK4* siRNA knockdown.

(C) MTT assay was conducted to evaluate the proliferation capacity of HUVECs between scramble siRNA and *EIF2AK4* siRNA groups during a 4-day time period. * $p < 0.05$ by two-way ANOVA followed by Bonferroni post hoc test.

(D) Representative images of Ki67 immunostaining and quantitative data to compare the proliferation capacity of HUVECs between scramble siRNA and *EIF2AK4* siRNA groups. Scale bar, 50 μm .

(E) Representative images of tube formation of HUVECs from scramble siRNA and *EIF2AK4* siRNA groups with quantitative analysis. Scale bar, 100 μm . Three independent experiments were performed in duplicate.

3-kinase (PI3K)-protein kinase B (AKT) signaling pathway (Figure 4B). These genes were regulated by the *EIF2AK4* compound heterozygous variants, and they were correlated with cell proliferation and angiogenesis, as presented in Figure 4C. Proliferating cell nuclear antigen (*PCNA*) and minichromosome maintenance (*MCM*) proteins are standard markers of proliferation that are commonly used to assess the growth fraction of a cell population (Juríková et al., 2016). In the present study, the *PCNA* and *MCM* proteins were obviously upregulated in PVOD-iPSC-ECs. It was speculated that the PI3K-Akt signaling pathway was the mainly disturbed pathway involved in the abnormal PVOD-iPSC-EC proliferation and angiogenesis (Haque and Morris, 2017; Wang et al., 2013). Therefore, the expressions of downstream genes were detected, and it was found that the components of the PI3K-AKT signaling pathway evidently changed, and that PVOD-iPSC-ECs expressed higher levels of pro-proliferation (*PCNA*, *MCM7*, and *MCM4*) and pro-angiogenesis genes (*PDGFD*, *VEGFA*, and *TNC*), and lower levels of anti-angiogenesis gene

ANGPTL1 (Yu et al., 2021) (Figure 4C). Phospho-Akt/Total-Akt expression was upregulated in PVOD-iPSC-ECs, when compared with GC-PVOD-iPSC-ECs, indicating activation of the AKT signaling (Figure 4D). The further real-time qPCR analysis validated the expression of genes correlated with proliferation (*PCNA*, *MCM7*, and *MCM4*) and angiogenic processes (*PDGFD*, *VEGFA*, *TNC*, and *ANGPTL1*) (Figures 4E and 4F). Overall, PVOD-specific-ECs were generated, and it was observed that *EIF2AK4* compound heterozygous variants contribute to the PVOD-iPSC-EC disease phenotype by regulating the transcriptional profiling correlated with cell proliferation and angiogenesis.

The inactivation of the PI3K/AKT signaling pathway is beneficial for PVOD-iPSC-ECs

We attempted to identify novel and effective targeted treatments based on the changes in the molecular biology in PVOD-iPSC-ECs and evaluated the therapeutic efficacy of AKT inhibitors AZD5363 and MK2206 on

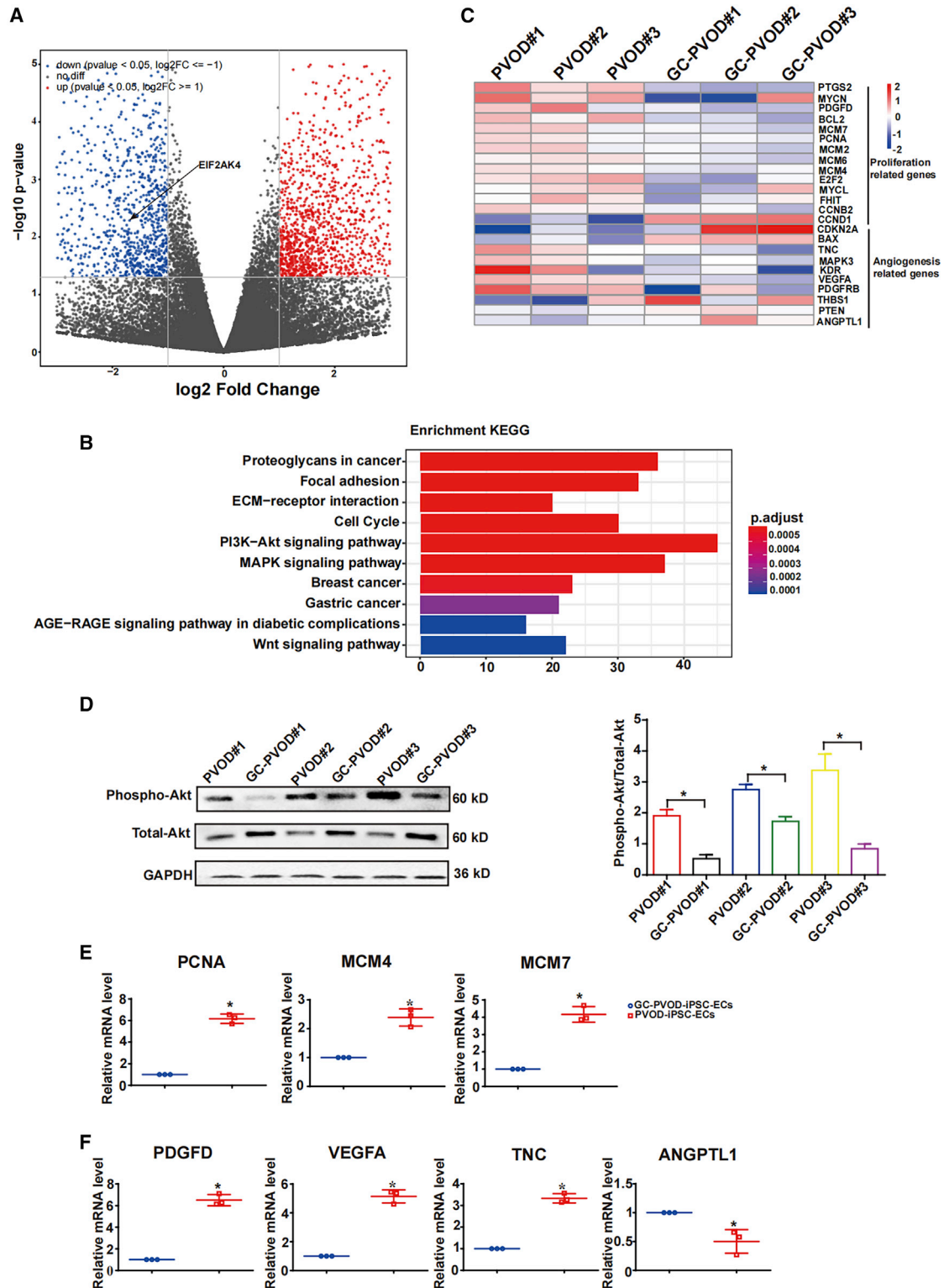


Figure 4. Differential mRNA-level expression of proliferation and angiogenesis in PVOD induced pluripotent stem cell-derived endothelial cells (iPSC-ECs)

(A) Volcano plots of genes in RNA sequencing between PVOD-iPSC-ECs and GC-PVOD-iPSC-ECs. Blue plots indicate the downregulated genes, and red plots indicate the upregulated genes.

(legend continued on next page)



PVOD-iPSC-ECs. AZD5363, which is also known as capivasertib, is an Akt signaling inhibitor that binds to and inhibits all Akt isoforms (Mroweh et al., 2021). MK2206, which is another allosteric Akt isoform small molecule inhibitor that has been studied *in vitro* and *in vivo* in various cancers, has exhibited interesting *in vitro* activity, resulting in cell-cycle arrest, the inhibition of cancer cell proliferation, and the promotion of apoptosis (Wilson et al., 2014). Remarkably, the Ki67 immunostaining indicated that both AZD5363 (8 nM) and MK2206 (10 μ M) have inhibitory effect on PVOD-iPSC-EC proliferation through both microscopic observation and quantitative analysis, when compared with the control group (Figures 5A and 5B). A similar trend was also confirmed in MTT assay that both AZD5363 and MK2206 have a significant dose-dependent inhibitory effect on PVOD-iPSC-EC proliferation, in a dose-dependent manner, during the 4-day time period (Figures 5C and 5D). After 24 h of 8 nM of AZD5363 treatment or 10 μ M of MK2206 treatment, the tube formation assay revealed a significant restrained effect on PVOD-iPSC-ECs, when compared with DMSO-treated cells, when observed under a microscope (Figure 5E). Furthermore, the AZD5363 and MK2206 treatment markedly attenuated the abnormal phenotype of PVOD-iPSC-ECs, accompanied by the decreased mRNA levels of proliferation markers (PCNA and MCM7) and angiogenesis markers (PDGFD and VEGFA) (Figures S4A and S4B). These data establish the AKT signaling as a novel therapeutic target for PVOD, indicating that AKT inhibitors may hold promise for the treatment of PVOD patients.

Imatinib and amifostine attenuate the disease phenotype of PVOD-iPSC-ECs

To date, despite the rapid advances in understanding the mechanisms and genetic basis of PVOD, much less is known on the treatments for PVOD patients. Imatinib is a tyrosine kinase inhibitor specific for platelet-derived growth factor receptor (PDGFR) (Demetri et al., 2002). Since PDGFR is highly expressed in smooth muscle cells of the pulmonary artery in patients with PAH (Montani et al., 2013), imatinib has been suggested as a treatment option for PAH patients (Galiè et al., 2005). Recently, a clinical trial reported that treatment with imatinib can prolong the lifetime and improve the functional capacity of clinically

diagnosed PVOD patients (Ogawa et al., 2017; Overbeek et al., 2008; Sato et al., 2019). However, the biological functions of imatinib have not been elucidated at present. In the present study, PVOD-iPSC-ECs were stimulated with imatinib, and MTT assay, Ki67 immunostaining, and tube formation assay were performed. As shown in Figure 6, imatinib significantly attenuated the disease phenotype of PVOD-iPSC-ECs. Accordingly, the mRNA levels of *PCNA*, *MCM7*, *PDGFD*, and *VEGFA* were obviously inhibited by imatinib (Figure S4C). Imatinib mainly signals through two receptors, *PDGFRA* and *c-Kit* (Belloc et al., 2009; Joensuu et al., 2017). The investigators further explored whether imatinib suppresses the PVOD-iPSC-EC proliferation and angiogenic capacity through *PDGFRA* and *c-Kit*, or both. Real-time qPCR showed mRNA levels of *PDGFRA* and *c-Kit* were significantly upregulated in PVOD-ECs (Figure S5A). As an important member of tyrosine kinase family, *c-kit* receptor causes specific expression of certain genes, regulates cell differentiation and proliferation, and resists cell apoptosis through activating the downstream signaling molecules fold-lowing interaction with stem cell factor (SCF). SCF/*c-kit* downstream signal transduction pathways are very complex, and currently known signal transduction pathways include *Ras/Erk*, *PI3K*, *PLC- γ* , and *JAK/STAT* (Liang et al., 2013), which have overlap with *PDGFRA* downstream signaling pathways. Therefore, it is indistinct to distinguish *SCF/c-kit* from *PDGFRA*. Whereas, nearly no change of SCF expression between PVOD-ECs and GC-PVOD-ECs (Figure S5A) implied no activation of *c-Kit* signaling. Additionally, AKT signaling is a downstream pathway of *PDGFRA*, and AKT activation was inhibited by imatinib (Figure S5B). Hence, we concluded imatinib may inhibit ECs proliferation by *PDGFRA* pathway.

Over the last 6 decades, amifostine has been pursued as the radioprotective agent of choice by diverse institutions, investigators, and government/funding agencies (Capizzi, 1999; Capizzi and Oster, 2000). A research reported that amifostine ameliorated the mitomycin-induced rat PVOD model with notable improvement in survival, right ventricle hypertrophy, and pulmonary hemodynamics (Perros et al., 2015). However, there are nearly no reports pertaining to the pharmacodynamic study of amifostine on PVOD patients. The present study assessed the effect of amifostine on PVOD-iPSC-ECs, and surprisingly, it was

(B) KEGG pathways analysis of genes regulated by EIF2AK4 compound heterozygous variants.

(C) Heatmap comparative analysis of genes related to proliferation and angiogenesis biological processes between PVOD-iPSC-ECs and GC-PVOD-iPSC-ECs.

(D) Phospho-AKT/total-AKT expression quantified by western blot and densitometric quantification in PVOD-iPSC-ECs and GC-PVOD-iPSC-ECs. * $p < 0.05$ by one-way ANOVA followed by the Bonferroni test. Three independent experiments were performed in duplicate.

(E and F) Real-time qPCR of representative genes related to proliferation and angiogenesis biological processes between PVOD-iPSC-ECs and GC-PVOD-iPSC-ECs. Including *PCNA*, *MCM7*, *MCM4*, *PDGFD*, *VEGFA*, *TNC*, and *ANGPTL1*. Data are presented as the mean \pm SEM. * $p < 0.05$ vs. GC-PVOD-iPSC-ECs by Student's *t* test. Three independent experiments were performed in duplicate.

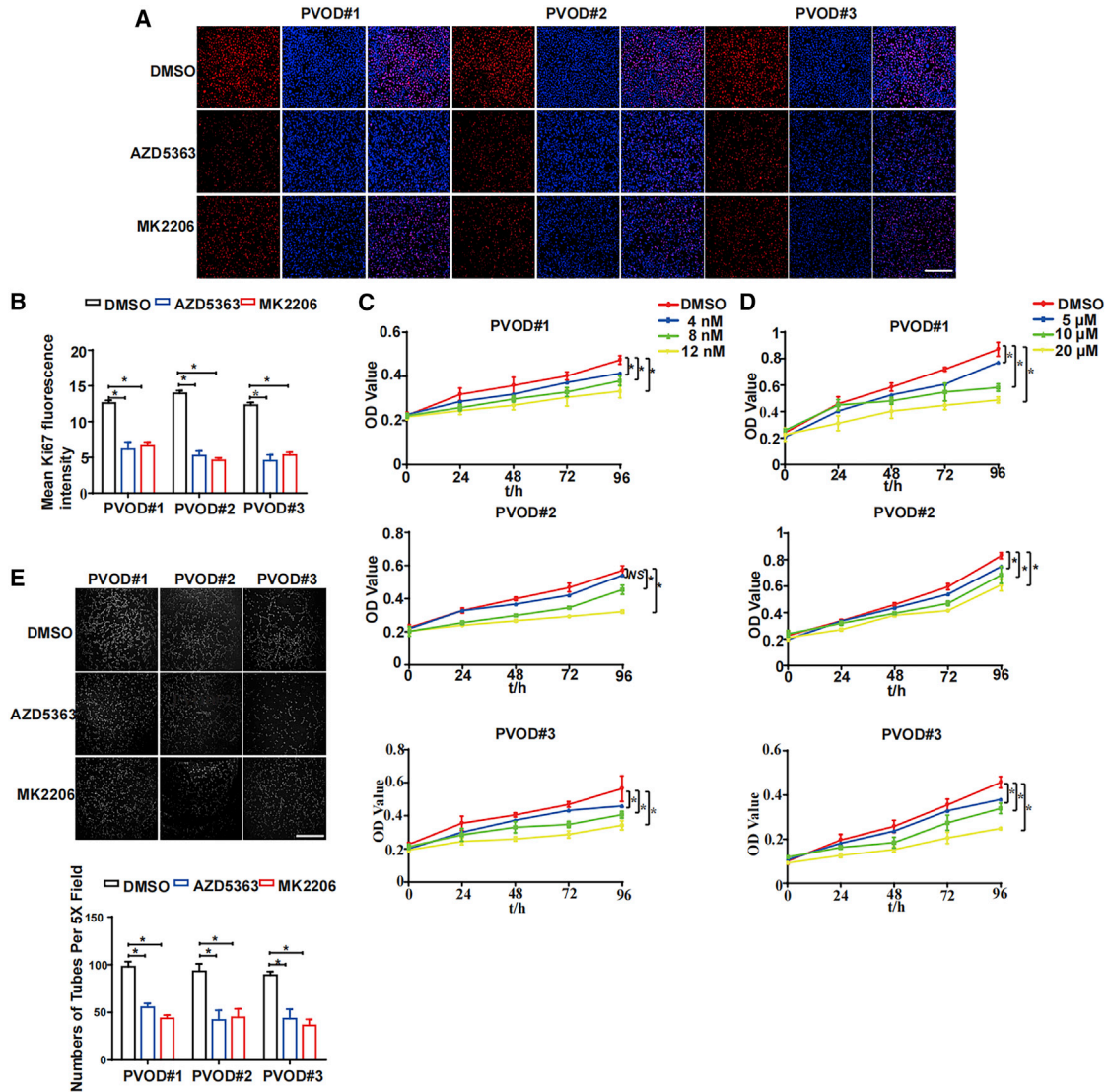


Figure 5. AZD5363 and MK2206 are beneficial to PVOD-iPSC-ECs disease phenotype with *EIF2AK4* compound heterozygous variants

(A and B) Representative images of Ki67 immunostaining of PVOD-iPSC-ECs with DMSO, 8 nM AZD5363, or 10 μM MK2206 treatment and quantitative analysis. Red: Ki67; blue: DAPI. Scale bar, 100 μm. Data are presented as the mean ± SEM. * $p < 0.05$ vs. DMSO group by Student's t test.

(C) MTT assay to assess the inhibitory effect of AZD5363 on PVOD-iPSC-ECs at dose-dependent concentration during a 4-day time period. * $p < 0.05$ vs. DMSO group. Two-way ANOVA followed by the Bonferroni post hoc test.

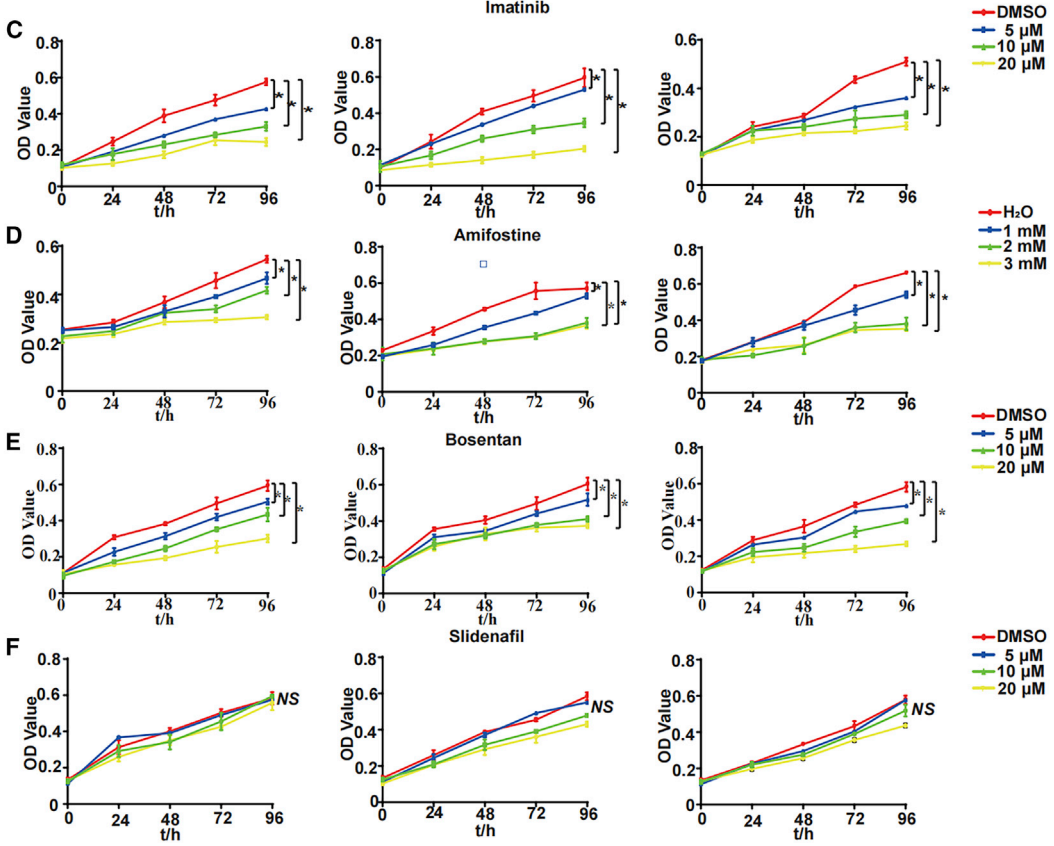
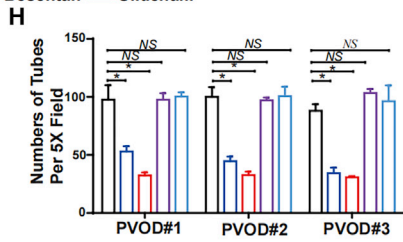
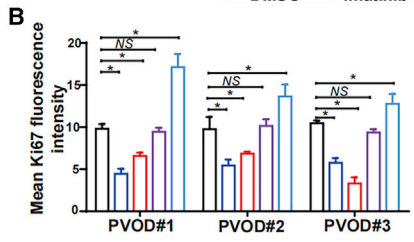
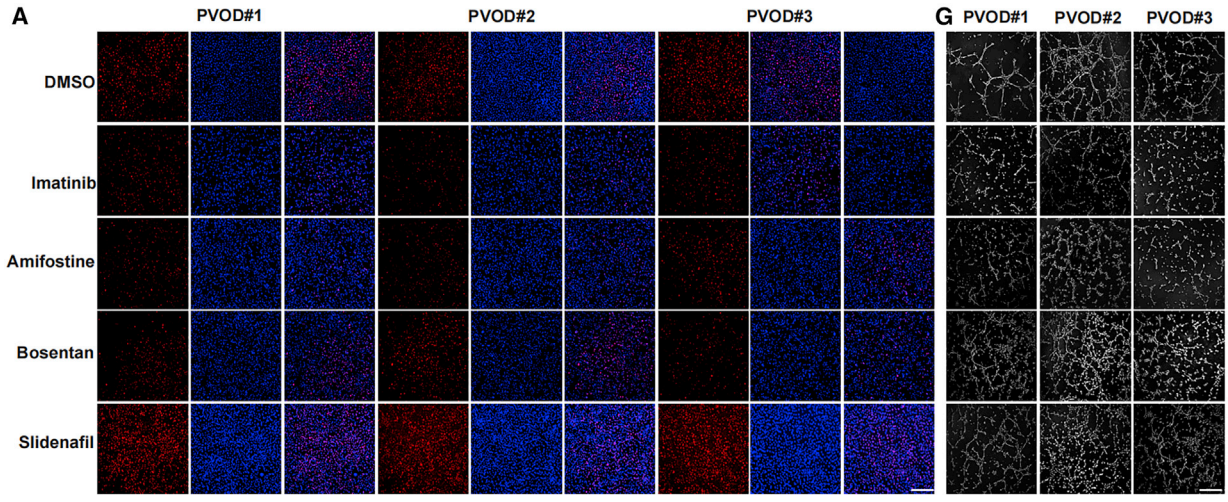
(D) MTT assay to assess the inhibitory effect of MK2206 on PVOD-iPSC-ECs at dose-dependent concentration during a 4-day time period. * $p < 0.05$ vs. DMSO group. Two-way ANOVA followed by the Bonferroni post hoc test.

(E) Representative images of tube formation of PVOD-iPSC-ECs with DMSO, 8 nM AZD5363, or 10 μM MK2206 treatment and quantitative analysis. Scale bar, 100 μm.

found that at 48 h, the 2 mM of amifostine markedly attenuated the proliferation and angiogenic capacity. As shown in Figure 6, the image suggests the preventive effect of amifostine. Therefore, the cytoprotective agent may be an appropriate candidate drug for PVOD patients. Meanwhile,

representative marker genes *PCNA*, *MCM7*, *PDGFD*, and *VEGFA* were suppressed with the amifostine treatment (Figure S4D).

The present results provide evidence that imatinib and amifostine can be alternative potential drugs for PVOD



(legend on next page)



patients, since these can apparently rescue the disease phenotype of ECs correlated with PVOD at the single-cell level, which are mainly involved in the PVOD pathological process.

The nonprotective effect of bosentan and sildenafil on PVOD-iPSC-ECs

Due to the similar clinical picture of dyspnea on exertion and signs of right heart failure, PVOD is difficult to distinguish from idiopathic PAH (Daraban et al., 2015). However, the administration of PAH-specific therapy (such as endothelin receptor antagonists and type 5 phosphodiesterase inhibitors) can precipitate severe acute pulmonary edema (Bhogal et al., 2019; McLaughlin et al., 2015a). As a synthesized dual endothelin receptor antagonist, bosentan acts as a vasodilator and an anti-proliferative agent, and it is the first oral agent available in China for the treatment of PAH (McLaughlin et al., 2015b; You et al., 2018). However, the clinical outcomes of PVOD patients were worse than those of PAH patients (Palmer et al., 1998; Resten et al., 2004). Although the underlying molecular mechanism remains unclear, the specific vascular endothelial cells obtained from the PVOD patient iPSC line in the present study made it possible to explore the impact of bosentan on ECs. Bosentan has a significant dose-dependent inhibitory effect on PVOD-iPSC-EC proliferation (Figures 6A and 6E). After 48 h of 10 μ M of bosentan treatment, the tube formation assay revealed the significant intensive effect of bosentan on PVOD-iPSC-ECs, when compared with DMSO-treated cells (Figures 6G and 6H), and this was accompanied by decreased levels of both PCNA and MCM7, while PDGFD and VEGFA were upregulated after the bosentan treatment (Figure S4E).

Another frequently used drug for PAH patients is sildenafil, which is a type 5 phosphodiesterase inhibitor that reduces pulmonary arterial pressure by increasing the levels of cGMP and nitric oxide in the pulmonary vasculature (Dhariwal and Bavdekar, 2015; Galiè et al., 2005). In a previous study, the patient developed acute pulmonary edema after the introduction of sildenafil (Duarte et al., 2020; Kuroda et al., 2006). We treated the PVOD-iPSC-ECs at 5, 10, and 20 μ M concentrations, and the results revealed that sildenafil exhibited a slight upregulation on PVOD-iPSC-EC proliferation capacity (Figures 6A and 6F). Furthermore,

the tube formation assay indicated that the tube formation capacity of the different groups was similar (Figures 6G and 6H). Moreover, the mRNA expression levels of PCNA, MCM7, PDGFD, and VEGFA exhibited nearly no differences between the control and sildenafil groups (Figure S4F). Overall, the results demonstrate that although bosentan and sildenafil are available for PAH patients, these may not be the optimal drugs for PVOD, since both could not completely reverse the malfunctional phenotype of PVOD-iPSC-ECs.

DISCUSSION

In the present study, an iPSC-based disease model was utilized, and iPSCs were generated from three PVOD patients who carried two compound heterozygous variants of the *EIF2AK4* gene and two healthy control subjects. Then, the p.Arg989Trp variant (c.2965C>T) in PVOD#1, p.Lys1154Ter variant (c.3460A>T) in PVOD#2, p.Pro1611fs variant (c.4832_4833insAAAG) in PVOD#3 were corrected by CRISPR-Cas9 technology in order to generate the GC-PVOD-iPSC lines. The PVOD-iPSC-ECs exhibited a decrease in *EIF2AK4* expression, both at the protein and mRNA levels. Furthermore, PVOD-iPSC-ECs exhibited a disease phenotype featured by excessive proliferation and increased tube formation capacity, when compared with control-iPSC-ECs and GC-PVOD-iPSC-ECs. This is consistent with the morphological observation obtained from PVOD human lung tissues or MMC-exposed rat lung tissues (Fabrice et al., 2015). Furthermore, the gene transcriptional profiling of iPSC-ECs exhibited changes correlated with cell proliferation and angiogenic capacity. The elucidation of the PVOD pathophysiology allows for the better understanding of the disease process and, consequently, the development of potential new therapies. Critically, the present results revealed that the disrupted proliferation and angiogenic phenotype of PVOD-iPSC-ECs were normalized by AKT inhibitor AZD5363 or MK2206, as shown in Figure 7. In addition, imatinib and amifostine both could alleviate the cellular disease phenotype, while bosentan and sildenafil could not. Even though they may be beneficial for PAH patients, they would frequently induce pneumonema when applied to PVOD patients.

Figure 6. Relative PAH-drugs testing on PVOD-iPSC-ECs

(A and B) Representative images of Ki67 immunostaining of PVOD-iPSC-ECs with DMSO, 10 μ M imatinib, 2 mM amifostine, 10 μ M bosentan, and 10 μ M sildenafil treatment and quantitative analysis. Scale bar, 100 μ m.

(C–F) MTT assay to assess the inhibitory effect of imatinib, amifostine, bosentan, and sildenafil on PVOD-iPSC-ECs at dose-dependent concentration during a 4-day time period.

(G and H) Representative images of tube formation of PVOD-iPSC-ECs with DMSO, amifostine, bosentan, and sildenafil treatment and quantitative analysis. Scale bar, 100 μ m. Data are presented as the mean \pm SEM. * $p < 0.05$ vs. DMSO group by Student's *t* test. Three independent experiments were performed in duplicate.

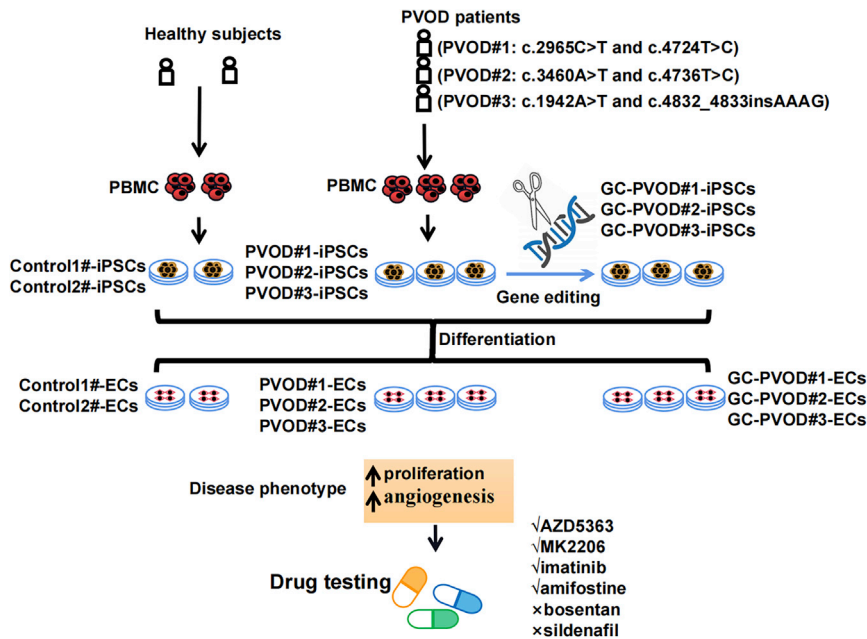


Figure 7. Mechanistic overview of the study

Normal iPSCs and patient-specific iPSCs are generated from two healthy subjects and three PVOD patients. CRISPR-Cas9 genome editing is used to correct the *EIF2AK4* variants. The normal iPSCs, PVOD-iPSCs, and GC-PVOD-iPSCs are differentiated into ECs. PVOD-iPSC-ECs exhibited disease phenotype featured by excessive proliferation and increased tube formation capacity when compared with those in control-iPSC-ECs and GC-PVOD-iPSC-ECs. Drug testing reveals that AZD5363, MK2206, imatinib, and amifostine, but not bosentan and sildenafil, normalize the disease phenotype of PVOD-iPSC-EC.

As reported in a previous research, merely the biallelic variants of *EIF2AK4* can cause heritable PVOD, while the heterozygous variant is insufficient. In order to provide more evidence for this presumption, the present study generated the GC-PVOD-iPSC lines as isogenic controls by erasing the specific variant sites. On one hand, the GC-PVOD-iPSC-ECs made it possible to eliminate the discrepancy caused by different genetic backgrounds, when compared with unrelated healthy individuals with a heterogeneously genetic background as the control. On the other hand, the phenotype of GC-PVOD-iPSC-ECs regressed to normal and strengthened the hypothesis that the biallelic variant of the *EIF2AK4* gene is the initiator for PVOD at the cellular level, further elucidating the cellular disease mechanism and effects of the tested drugs.

GCN2(*EIF2AK4*) belongs to a family of four kinases and phosphorylates the α -subunit of eukaryotic translation initiation factor 2 (eIF2 α). Phosphorylation of eIF2 α protects cells by reducing protein synthesis to maintain the homeostasis. We speculated the decreased expression of GCN2 caused by *EIF2AK4* mutations breaks the equilibrium and leads to excessive proliferation of ECs. Recently, Li et al.'s study indicated that GCN2 deletion led to activation of the AKT/mTOR pathway (Li et al., 2022), which is consistent with our conclusion in this study. Additionally, they showed GCN2 maintained proteostasis and inhibited Src-mediated AKT activation. Src is a tyrosine kinase that interacts with and facilitates AKT phosphorylation. We assumed that *EIF2AK4* mutations activated the AKT signaling by upregulating Src in endothelial cells, and

PVOD-ECs were treated with Scr inhibitor PP2. As shown in Figure S5C, PP2 efficiently inhibited the phosphorylation of Akt.

A defining pathological feature of PVOD is the diffuse involvement of venules and septal veins in a vasculopathy characterized by intimal fibrosis resulting in luminal narrowing or obliteration (Pietra et al., 2004; Wagenvoort and Wagenvoort, 1974). To observe endothelial to mesenchymal transition (EMT) in PVOD-iPSC-ECs, we performed real-time PCR of EMT target genes and immunofluorescence of α -SMA. As shown in Figure S6, mRNA levels of Twist1 and ID1 had nearly no change between control and three PVOD-iPSC-ECs lines (Figure S6A), and α -SMA had negative staining in PVOD-iPSC-ECs (Figure S6B). Therefore, to date, there has been no significant evidence illustrating EMT in this study.

Actually, we also corrected *EIF2AK4* c.4724 T>C variant in PVOD#1, c.4736T>C variant in PVOD#2, and c.1942 T>C variant in PVOD#3 and obtained double-mutation corrected iPSC-ECs as control. When compared with double-mutation corrected iPSC-ECs, PVOD-iPSC-ECs still showed a decreased in *EIF2AK4* expression and exhibited a typical disease phenotype featured by excessive proliferation and increased tube formation capacity (Figure S7).

In clinic, there are nearly no drugs available for the accurate treatment of PVOD. Another finding in the present study was the identification of AKT inhibitors. Both AZD5363 and MK2206 were effective for reversing the disease phenotype of PVOD-iPSC-ECs. The PI3K/Akt signaling is crucial to various aspects of cell growth and survival, and



it is one of the most frequently hyperactivated signaling pathways in cancer cells. Therefore, Akt inhibitors have been extensively considered as therapeutic agents for cancers (Alzahrani, 2019; Porta et al., 2014). Present evidence supports the concept that PVOD and pulmonary capillary hemangiomatosis have indeed a varied expression of the same disorder, and that biallelic mutations in the *EIF2AK4* gene are responsible for both (Alzahrani, 2019). Apparently, the changed behaviors of pulmonary endothelial cell caused by the *EIF2AK4* biallelic variants are similar to those in cancer cells. However, further detailed investigations are needed to determine whether other therapeutic drugs for cancer patients are appropriate for PVOD patients.

iPSCs potentially provide an opportunity to generate a human cell-based model of PVOD to test the effects of PAH-related drugs. Even at the cellular level, both imatinib and amifostine can obviously inhibit the effect on cell proliferation and angiogenic capacity at appropriate concentrations. However, it remains difficult to extrapolate this from *in vitro* studies, due to the complete organism where the intricate factors are involved, such as the hemodynamics status, lung vasculature, and vascular remodeling. Therefore, it remains to be determined whether imatinib and amifostine toxins may be used as therapeutic drugs for the treatment of PVOD in clinic in the future. Indeed, further investigations on safety and efficacy on humans are also needed, especially for amifostine, which has never been used in humans. To date, there has been a paucity of data on the therapeutic schedule of this rare disease. These present findings provide evidence that illustrates the different responses of PVOD-iPSC-ECs to the aforementioned medicines, suggesting a theoretical basis for clinical medication on PVOD patients.

The present study has some limitations. First, the low yield and significant heterogeneity of the observed ECs were the notable defects of the differentiation technique. In addition, when compared with adult pulmonary vein endothelial cells *in vivo*, the maturity of iPSC-ECs still needs to be improved through further studies in order to allow these to accurately respond to different stimulates. Second, we attempted to utilize a credible and reasonable animal model capable of imitating the pathologic mechanism of human PVOD caused by *EIF2AK4* biallelic mutations in order to decipher the previous observations from iPSC-derived ECs. Regrettably, merely the PVOD animal model developed by Frédéric Perros was induced by mitomycin, which involved a totally different pathogenic mechanism, in which even the GCN2 expression decreased. Hence, this was not suitable for *in vitro* studies in the present research. Meanwhile, we collected information that the *EIF2AK4*^{-/-} mouse does not display PVOD phenotype and shows no defects in car-

diovascular system and respiratory system from The Mouse Genome Informatics Database (MGD; <http://www.informatics.jax.org>) which is a community model organism knowledgebase for the laboratory mouse (Blake et al., 2021). Furthermore, the discrepancy between multi-species and environmental impact for mutation penetrance may explain for that. Third, the iPSC-ECs or HUVECs used in the present study were not lung specific. Hence, it was not fully convincing to explain why pulmonary vessels were more susceptible to *EIF2AK4* mutations. GCN2 is an eIF2 α kinase responsible for entirely rewiring the metabolism of cells in response to amino acid starvation stress, and it has been demonstrated that >10% of cancer cell lines appear to be dependent on GCN2 (Saavedra-García et al., 2021) (Gold and Masson, 2022). The factors in the lung environment that trigger the disease require further longitudinal studies.

Collectively, these present findings demonstrate that patient-specific PVOD-iPSC-ECs and GC-PVOD-iPSC-ECs are able to recapitulate the single-cell phenotype of PVOD caused by *EIF2AK4* loss-of-function variants. These latest insights into the pathology of PVOD may help elucidate the underlying mechanism and discover suitable therapeutic drugs for treating this disease.

EXPERIMENTAL PROCEDURES

Resource availability

Corresponding author

Further information and requests for resources and reagents should be directed to and will be fulfilled by the corresponding author, Zhou Zhou (fwcomd@126.com).

Materials availability

This study did not generate new unique reagents.

Data and code availability

RNA-seq data have been deposited in the NCBI Gene Expression Omnibus. The accession number for the RNA-seq data reported in this paper is GEO: GSE215978.

Materials

The following antibodies were used: goat antibody against human VE-cadherin (1:1,000, AF938; R&D systems); rabbit antibody against human GCN2 (1:1,000; ab134053; Abcam); rabbit antibody against human NANOG (1:500; ab109250; Abcam); rabbit antibody against human OCT4 (1:500; ab200834; Abcam); mouse antibody against human SSEA-1 (1:500; ab16285; Abcam); mouse antibody against human TRA-1 (1:500; ab16288; Abcam); rabbit antibody against phospho-Akt (Ser473) (1:1,000; 31957; Cell Signaling); rabbit antibody against Akt (pan) (1:2,000; 4691; Cell Signaling); Ki67 rabbit monoclonal antibody (1:200; AF1738, Beyotime); Alexa Fluor 488-conjugated donkey anti-rabbit IgG (1:1,000; R37118; Life Technologies); Ficoll-Paque PREMIUM sterile solution (17544202; GE Healthcare); CytoTune-iPS 2.0 Sendai Reprogramming Kit (A16517; Thermo Fisher



Scientific); Matrigel (354277; BD); mTeSR medium (05850; STEMCELL Technologies); Y-27632 (STEMCELL Technologies); Accutase (07920; STEMCELL Technologies); MTT for cell proliferation detection (C0009S; Beyotime).

Patient recruitment

Human samples were collected after written informed consent according to the declaration of Helsinki and local ethics board approval (Approval No. 2017-877). PBMCs were obtained from three PVOD patients and two healthy control subjects, and they all signed the informed consent. This study was approved by the Ethics Committees of Fuwai Hospital, National Center for Cardiovascular Diseases, China.

Gene correction of *EIF2AK4* variant site by CRISPR-Cas9

Isogenic gene-corrected control was generated using CRISPR-Cas9 mediated homology-directed repair with single-stranded oligo DNA nucleotide (ssODN), which provided the wild-type template for gene correction. To correct the heterozygous c.2965C>T (p. Arg989Trp) mutation in exon 21, the c.3460A>T mutation (p. Lys1154Ter) in exon 25, and the c.4832_4833insAAAG (p. Pro1611fs) in exon 38 of *EIF2AK4* gene, three mutation-specific sgRNA, termed sgEIF2AK4 (target site: GTGGCTGTGGCCAT TTGC, ATTTCATCCCTAAGAAGCTTC, TGAGGTATCTTGCTTT CTT), were designed using CRISPOR in <http://crispor.tefor.net/>. SgEIF2AK4 were generated by *in vitro* transcription using GeneArt Precision gRNA Synthesis Kit (Thermo Fisher Scientific) according to the manufacturer's instructions. ssODN was designed to contain 125 nt in total. The sequences of ssODNs are listed in Table S2. PVOD-iPSCs at 70%–80% confluence were harvested with 0.5 mM EDTA. 1.0×10^5 cells were co-electroporated with 400 ng sgEIF2AK4, 2 μ g recombinant Cas9 protein (Thermo Fisher Scientific), and 10 pmol ssODN using 10 μ L Neon Tip with 1,100 V, 20 ms, and two pulses by Neon transfection system (Thermo Fisher Scientific). Immediately after electroporation, cells were transferred into one well of Matrigel-coated 24-well plate and cultured in 500 μ L mTeSR1 medium containing 5 μ M Y-27632 (Selleck Chemicals). Medium was changed daily and Y-27632 was removed 24 h later. 3 days after electroporation, cells were dispersed at low density into Matrigel-coated 60-mm dish in mTeSR1 medium with 10 μ M Y-27632, which was removed 24 h later. About 14 days later, large colonies were picked and expanded, which were analyzed for the desired base correction by sanger sequencing of amplicon spanning the target site of *EIF2AK4* gene. A positive clone was selected for further analysis.

Endothelial cell differentiation

iPSC-ECs were generated using a 2D monolayer differentiation protocol based on a modification of a previous protocol by Gu's group (Gu, 2018). Briefly, iPSCs (over passage 25) were grown to 80% confluence and placed in differentiation medium (RPMI and B-27 supplement minus insulin, Life Technologies) toward the mesodermal lineage with 6 mM CHIR-99021 (Selleck Chemicals) for 2 days, followed by 3 mM CHIR-99021 for 2 days. The medium was then changed to a differentiation medium composed of RPMI-B27 without insulin and endothelial medium

EGM2 (Lonza Group) supplemented with 20 ng/mL bone morphogenetic protein-4 (PeproTech), 50 ng/mL vascular endothelial growth factor (PeproTech), and 20 ng/mL basic fibroblast growth factor (BD Biosciences). Cells were subjected to medium change every 2 days. On day 12, iPSC-ECs were sorted for CD144+ using antibody-coated beads and a magnetic-activated cell sorter (Miltenyi Biotec) and expanded on 0.2% gelatin coated plates and maintained in EGM-2 BulletKit (Lonza Group) with 10 μ M SB431542 (Selleck Chemicals), a TGF- β inhibitor at 37°C, 21% O₂, and 5% CO₂ in a humidified incubator with medium changes every 48 h. Cells were passaged once they reached 80%–90% confluence. iPSC-ECs used for experiments were between passages 3 and 10.

Statistical analysis

All data are presented as the mean \pm standard error of the mean (SEM). The statistical analyses were performed using GraphPad Prism 8.0 software (San Diego). For statistical comparisons, we first used a normality test to evaluate whether the data were normally distributed. For two-group comparisons of normally distributed data, we applied Student's *t* test with Welch's correction if equal standard deviations were not assumed through an *F* test. In addition, the Brown-Forsythe test was used to assess equal variances among data from more than two groups; we applied ordinary ANOVA or Welch ANOVA for equal variances assumed or not, respectively. Nonparametric tests were used when the data were not normally distributed. In all cases, a statistically significant difference was present when the two-tailed probability was less than 0.05. The details of the statistical analysis applied to each experiment are presented in the corresponding figure legends.

SUPPLEMENTAL INFORMATION

Supplemental information can be found online at <https://doi.org/10.1016/j.stemcr.2022.10.014>.

ACKNOWLEDGMENTS

We thank the PVOD patients for kindly providing fresh blood for obtaining PBMCs. This study was supported by the grant National Natural Science Foundation of China (no. 82000342).

AUTHOR CONTRIBUTIONS

Z.Z., C.X., and B.M. conceived the idea and designed the experiments. T.L. and W.L. performed the data analysis. B.M. prepared the manuscript. Q.Z. and C.X. are responsible for obtaining the PBMCs from the PVOD patients. Cell culture experiments were done by Z.P., H.Y., and K.W. The collection and assembly of the data were done by T.L., W.L. B.M. and Q.C. performed the iPSC differentiation and functional assays of the iPSC-ECs. T.L. and H.Y. contributed to the molecular experiments. Z.P. and K.W. helped with the revisions. All of the authors read and approved the final manuscript.

CONFLICT OF INTERESTS

The authors declare no competing interests.



Received: April 15, 2022
Revised: October 20, 2022
Accepted: October 20, 2022
Published: November 17, 2022

REFERENCES

- Alzahrani, A.S. (2019). PI3K/Akt/mTOR inhibitors in cancer: at the bench and bedside. *Semin. Cancer Biol.* *59*, 125–132.
- Belloc, F., Airiau, K., Jeanneteau, M., Garcia, M., Guérin, E., Lippert, E., Moreau-Gaudry, F., and Mahon, F.X. (2009). The stem cell factor-c-KIT pathway must be inhibited to enable apoptosis induced by BCR-ABL inhibitors in chronic myelogenous leukemia cells. *Leukemia* *23*, 679–685.
- Bhogal, S., Khraisha, O., Al Madani, M., Treece, J., Baumrucker, S.J., and Paul, T.K. (2019). Sildenafil for pulmonary arterial hypertension. *Am. J. Ther.* *26*, e520–e526.
- Blake, J.A., Baldarelli, R., Kadin, J.A., Richardson, J.E., Smith, C.L., and Bult, C.J.; Mouse Genome Database Group (2021). Mouse genome Database (MGD): knowledgebase for mouse-human comparative biology. *Nucleic Acids Res.* *49*, D981–D987.
- Capizzi, R.L. (1999). The preclinical basis for broad-spectrum selective cytoprotection of normal tissues from cytotoxic therapies by amifostine. *Semin. Oncol.* *26*, 3–21.
- Capizzi, R.L., and Oster, W. (2000). Chemoprotective and radioprotective effects of amifostine: an update of clinical trials. *Int. J. Hematol.* *72*, 425–435.
- Castilho, B.A., Shanmugam, R., Silva, R.C., Ramesh, R., Himme, B.M., and Sattlegger, E. (2014). Keeping the eIF2 alpha kinase Gcn2 in check. *Biochim. Biophys. Acta* *1843*, 1948–1968.
- Daraban, A.M., Enache, R., Predescu, L., Platon, P., Constantinescu, T., Mihai, C., Coman, I.M., Ginghina, C., and Jurcuș, R. (2015). Pulmonary veno-occlusive disease: a rare cause of pulmonary hypertension in systemic sclerosis. Case presentation and review of the literature. *Rom. J. Intern. Med.* *53*, 175–183. <https://doi.org/10.1515/rjim-2015-0024>.
- Demetri, G.D., von Mehren, M., Blanke, C.D., Van den Abbeele, A.D., Eisenberg, B., Roberts, P.J., Heinrich, M.C., Tuveson, D.A., Singer, S., Janicek, M., et al. (2002). Efficacy and safety of imatinib mesylate in advanced gastrointestinal stromal tumors. *N. Engl. J. Med.* *347*, 472–480.
- Dhariwal, A.K., and Bavdekar, S.B. (2015). Sildenafil in pediatric pulmonary arterial hypertension. *J. Postgrad. Med.* *61*, 181–192.
- Donnelly, N., Gorman, A.M., Gupta, S., and Samali, A. (2013). The eIF2 α kinases: their structures and functions. *Cell. Mol. Life Sci.* *70*, 3493–3511.
- Duarte, A.C., Cordeiro, A., Loureiro, M.J., and Ferreira, F. (2020). Pulmonary veno-occlusive disease: a probably underdiagnosed cause of pulmonary hypertension in systemic sclerosis. *Clin. Rheumatol.* *39*, 1687–1691.
- Eyries, M., Montani, D., Girerd, B., Perret, C., Leroy, A., Lonjou, C., Chelghoum, N., Coulet, F., Bonnet, D., Dorfmueller, P., et al. (2014). EIF2AK4 mutations cause pulmonary veno-occlusive disease, a recessive form of pulmonary hypertension. *Nat. Genet.* *46*, 65–69.
- Fabrice, A., Benoît, R., Valérie, N., Lau, E., Sébastien, B., and Frédéric, P. (2015). A simple method to assess in vivo proliferation in lung vasculature with EdU: the case of MMC-induced PVOD in rat. *Anal. Cell Pathol.* *2015*, 326385.
- Galiè, N., Ghofrani, H.A., Torbicki, A., Barst, R.J., Rubin, L.J., Badesch, D., Fleming, T., Parpia, T., Burgess, G., Branzi, A., et al. (2005). Sildenafil citrate therapy for pulmonary arterial hypertension. *N. Engl. J. Med.* *353*, 2148–2157.
- Galiè, N., Humbert, M., Vachiery, J.L., Gibbs, S., Lang, I., Torbicki, A., Simonneau, G., Peacock, A., Vonk Noordegraaf, A., Beghetti, M., et al. (2016). 2015 ESC/ERS guidelines for the diagnosis and treatment of pulmonary hypertension: the joint task force for the diagnosis and treatment of pulmonary hypertension of the European society of cardiology (ESC) and the European respiratory society (ERS): endorsed by: association for European paediatric and congenital cardiology (AEPC), international society for heart and lung transplantation (ISHLT). *Eur. Heart J.* *37*, 67–119.
- Gold, L.T., and Masson, G.R. (2022). GCN2: roles in tumour development and progression. *Biochem. Soc. Trans.* *50*, 737–745.
- Gu, M. (2018). Efficient differentiation of human pluripotent stem cells to endothelial cells. *Curr. Protoc. Hum. Genet.*, e64.
- Gu, M., Shao, N.Y., Sa, S., Li, D., Termglinchan, V., Ameen, M., Karakikes, I., Sosa, G., Grubert, F., Lee, J., et al. (2017). Patient-specific iPSC-derived endothelial cells uncover pathways that protect against pulmonary hypertension in BMPR2 mutation carriers. *Cell Stem Cell* *20*, 490–504.e5.
- Guo, F., Sun, Y., Wang, X., Wang, H., Wang, J., Gong, T., Chen, X., Zhang, P., Su, L., Fu, G., et al. (2019). Patient-specific and gene-corrected induced pluripotent stem cell-derived cardiomyocytes elucidate single-cell phenotype of short QT syndrome. *Circ. Res.* *124*, 66–78.
- Haque, S., and Morris, J.C. (2017). Transforming growth factor- β : a therapeutic target for cancer. *Hum. Vaccines Immunother.* *13*, 1741–1750.
- Joensuu, H., Wardelmann, E., Sihto, H., Eriksson, M., Sundby Hall, K., Reichardt, A., Hartmann, J.T., Pink, D., Cameron, S., Hohenberger, P., et al. (2017). Effect of KIT and PDGFRA mutations on survival in patients with gastrointestinal stromal tumors treated with adjuvant imatinib: an exploratory analysis of a randomized clinical trial. *JAMA Oncol.* *3*, 602–609.
- Juríková, M., Danihel, Ľ., Polák, Š., and Varga, I. (2016). Ki67, PCNA, and MCM proteins: markers of proliferation in the diagnosis of breast cancer. *Acta Histochem.* *118*, 544–552.
- Kuroda, T., Hirota, H., Masaki, M., Sugiyama, S., Oshima, Y., Terai, K., Ito, A., and Yamauchi-Takahara, K. (2006). Sildenafil as adjunct therapy to high-dose epoprostenol in a patient with pulmonary veno-occlusive disease. *Heart Lung Circ.* *15*, 139–142.
- Li, C., Wu, B., Li, Y., Chen, J., Ye, Z., Tian, X., Wang, J., Xu, X., Pan, S., Zheng, Y., et al. (2022). Amino acid catabolism regulates hematopoietic stem cell proteostasis via a GCN2-eIF2 α axis. *Cell Stem Cell* *29*, 1119–1134.e7.
- Liang, J., Wu, Y.L., Chen, B.J., Zhang, W., Tanaka, Y., and Sugiyama, H. (2013). The C-kit receptor-mediated signal transduction and tumor-related diseases. *Int. J. Biol. Sci.* *9*, 435–443.



- Manaud, G., Nossent, E.J., Lambert, M., Ghigna, M.R., Boët, A., Vihnhas, M.C., Ranchoux, B., Dumas, S.J., Courboulain, A., Girerd, B., et al. (2020). Comparison of human and experimental pulmonary veno-occlusive disease. *Am. J. Respir. Cell Mol. Biol.* *63*, 118–131.
- Mandel, J., Mark, E.J., and Hales, C.A. (2000). Pulmonary veno-occlusive disease. *Am. J. Respir. Crit. Care Med.* *162*, 1964–1973.
- Matsa, E., Burrridge, P.W., and Wu, J.C. (2014). Human stem cells for modeling heart disease and for drug discovery. *Sci. Transl. Med.* *6*, 239ps236.
- McLaughlin, V., Channick, R.N., Ghofrani, H.A., Lemarié, J.C., Naeije, R., Packer, M., Souza, R., Tapson, V.F., Tolson, J., Al Hiti, H., et al. (2015a). Bosentan added to sildenafil therapy in patients with pulmonary arterial hypertension. *Eur. Respir. J.* *46*, 405–413.
- McLaughlin, V.V., Shah, S.J., Souza, R., and Humbert, M. (2015b). Management of pulmonary arterial hypertension. *J. Am. Coll. Cardiol.* *65*, 1976–1997. <https://doi.org/10.1016/j.jacc.2015.03.540>.
- Montani, D., Günther, S., Dorfmueller, P., Perros, F., Girerd, B., Garcia, G., Jaïs, X., Savale, L., Artaud-Macari, E., Price, L.C., et al. (2013). Pulmonary arterial hypertension. *Orphanet J. Rare Dis.* *8*, 97. <https://doi.org/10.1186/1750-1172-8-97>.
- Montani, D., Lau, E.M., Dorfmueller, P., Girerd, B., Jaïs, X., Savale, L., Perros, F., Nossent, E., Garcia, G., Parent, F., et al. (2016). Pulmonary veno-occlusive disease. *Eur. Respir. J.* *47*, 1518–1534.
- Montani, D., Price, L.C., Dorfmueller, P., Achouh, L., Jaïs, X., Yaïci, A., Sitbon, O., Musset, D., Simonneau, G., and Humbert, M. (2009). Pulmonary veno-occlusive disease. *Eur. Respir. J.* *33*, 189–200.
- Mroweh, M., Roth, G., Decaens, T., Marche, P.N., Lerat, H., and Macek Jílková, Z. (2021). Targeting Akt in hepatocellular carcinoma and its tumor microenvironment. *Int. J. Mol. Sci.* *22*, 1794.
- Ogawa, A., Miyaji, K., and Matsubara, H. (2017). Efficacy and safety of long-term imatinib therapy for patients with pulmonary veno-occlusive disease and pulmonary capillary hemangiomatosis. *Respir. Med.* *131*, 215–219.
- Overbeek, M.J., Groepenhoff, H., Voskuyl, A.E., Smit, E.F., Peeters, J.W.L., Vonk-Noordegraaf, A., Spreeuwenberg, M.D., Dijkmans, B.C., and Boonstra, A. (2008). Membrane diffusion- and capillary blood volume measurements are not useful as screening tools for pulmonary arterial hypertension in systemic sclerosis: a case control study. *Respir. Res.* *9*, 68.
- Paik, D.T., Tian, L., Lee, J., Sayed, N., Chen, I.Y., Rhee, S., Rhee, J.W., Kim, Y., Wirka, R.C., Buikema, J.W., et al. (2018). Large-scale single-cell RNA-seq reveals molecular signatures of heterogeneous populations of human induced pluripotent stem cell-derived endothelial cells. *Circ. Res.* *123*, 443–450.
- Palmer, S.M., Robinson, L.J., Wang, A., Gossage, J.R., Bashore, T., and Tapson, V.F. (1998). Massive pulmonary edema and death after prostacyclin infusion in a patient with pulmonary veno-occlusive disease. *Chest* *113*, 237–240.
- Perros, F., Günther, S., Ranchoux, B., Godinas, L., Antigny, F., Chaumais, M.C., Dorfmueller, P., Hautefort, A., Raymond, N., Savale, L., et al. (2015). Mitomycin-induced pulmonary veno-occlusive disease: evidence from human disease and animal models. *Circulation* *132*, 834–847.
- Pietra, G.G., Capron, F., Stewart, S., Leone, O., Humbert, M., Robbins, I.M., Reid, L.M., and Tuder, R.M. (2004). Pathologic assessment of vasculopathies in pulmonary hypertension. *J. Am. Coll. Cardiol.* *43*, 25s–32s.
- Porta, C., Paglino, C., and Mosca, A. (2014). Targeting PI3K/Akt/mTOR signaling in cancer. *Front. Oncol.* *4*, 64.
- Resten, A., Maitre, S., Humbert, M., Rabiller, A., Sitbon, O., Capron, F., Simonneau, G., and Musset, D. (2004). Pulmonary hypertension: CT of the chest in pulmonary venoocclusive disease. *AJR Am. J. Roentgenol.* *183*, 65–70.
- Saavedra-García, P., Roman-Trufero, M., Al-Sadah, H.A., Blighe, K., López-Jiménez, E., Christoforou, M., Penfold, L., Capece, D., Xiong, X., Miao, Y., et al. (2021). Systems level profiling of chemotherapy-induced stress resolution in cancer cells reveals druggable trade-offs. *Proc. Natl. Acad. Sci. USA* *118*. e2018229118.
- Sato, H., Sugimura, K., Miura, M., Konno, R., Kozu, K., Yaoita, N., Shimizu, T., Yamamoto, S., Aoki, T., Tatebe, S., et al. (2019). Beneficial effects of imatinib in a patient with suspected pulmonary veno-occlusive disease. *Tohoku J. Exp. Med.* *247*, 69–73.
- Simonneau, G., Gatzoulis, M.A., Adatia, I., Celermajer, D., Denton, C., Ghofrani, A., Gomez Sanchez, M.A., Krishna Kumar, R., Landzberg, M., Machado, R.F., et al. (2013). Updated clinical classification of pulmonary hypertension. *J. Am. Coll. Cardiol.* *62*, D34–D41.
- Wagenvoort, C.A., and Wagenvoort, N. (1974). The pathology of pulmonary veno-occlusive disease. *Virchows Arch. A Pathol. Anat. Histol.* *364*, 69–79.
- Wang, X., Abraham, S., McKenzie, J.A.G., Jeffs, N., Swire, M., Tripathi, V.B., Luhmann, U.F.O., Lange, C.A.K., Zhai, Z., Arthur, H.M., et al. (2013). LRG1 promotes angiogenesis by modulating endothelial TGF- β signalling. *Nature* *499*, 306–311.
- Wilson, J.M., Kunnimalaiyaan, S., Gamblin, T.C., and Kunnimalaiyaan, M. (2014). MK2206 inhibits hepatocellular carcinoma cellular proliferation via induction of apoptosis and cell cycle arrest. *J. Surg. Res.* *191*, 280–285.
- Yang, H., Zeng, Q., Ma, Y., Liu, B., Chen, Q., Li, W., Xiong, C., and Zhou, Z. (2018). Genetic analyses in a cohort of 191 pulmonary arterial hypertension patients. *Respir. Res.* *19*, 87.
- You, R., Qian, X., Tang, W., Xie, T., Zeng, F., Chen, J., Zhang, Y., and Liu, J. (2018). Cost effectiveness of bosentan for pulmonary arterial hypertension: a systematic review. *Can. Respir. Res.* *2018*, 1015239.
- Yu, S., You, X., Liang, H., Li, Y., Fu, Y., Zhang, X., Hu, X., An, J., Xu, Y., and Li, F. (2021). First trimester placental mesenchymal stem cells improve cardiac function of rat after myocardial infarction via enhanced neovascularization. *Heliyon* *7*, e06120.